Industrial Crops & Products 171 (2021) 113868

Contents lists available at ScienceDirect

Industrial Crops & Products

journal homepage: www.elsevier.com/locate/indcrop

Sustainable production process of mechanically prepared nanocellulose from hardwood and softwood: A comparative investigation of refining energy consumption at laboratory and pilot scale

Wriju Kargupta [a], Reanna Seifert [b], Mark Martinez [b], James Olson [b], Joanne Tanner [a], Warren Batchelor [a,*]

[a] Bioresource Processing Research Institute of Australia (BioPRIA), Department of Chemical Engineering, Monash University, VIC, 3800, Australia
[b] Pulp and Paper Centre, The University of British Columbia, 321-2385 East Mall, Vancouver, BC, V6T 1Z4, Canada

ARTICLE INFO

Keywords:
Quality index
Refining
Energy efficiency
Nanocellulose
Hardwood
Softwood

ABSTRACT

In the drive towards sustainable development, the growing application of renewable, biodegradable, green materials to substitute non-renewable resources has roused substantial interest. However, the very high electrical energy consumption typical of mechanical nanocellulose production is a significant drawback, from the point of view of both environmental impact and production cost. The aim of this study was to investigate the effect of fiber source, mechanical treatment mode and scale on the energy consumption for nanocellulose production. Nanocellulose (mechanically prepared fibers), also known as cellulose nanofibers, or CNF) from hardwood eucalyptus (*Eucalyptus grandis*) and northern bleached softwood which is believed to be a mix of lodgepole pine (*Pinus contorta)* and white spruce (*Picea glauca*) pulp was prepared using lab scale and pilot scale mechanical refiners. The rate of increase in fiber aspect ratio confirms that disc (pilot scale) refining is seven and thirty-three times more energy efficient than lab scale PFI (Papir Forsknings Institutet) mill refining for processing softwood and hardwood, respectively. A novel quality index (Q) is proposed which considers the percentage of fines, fiber diameter and relative bonded area in the sheet to demonstrate the production of high quality nanocellulose. When the energy required to reach equivalent values of Q were compared, it was found that pilot disc refining of hardwood is approximately fifty-eight times more energy efficient than laboratory PFI mill refining of softwood. Fines generation for hardwood and softwood was fifteen and eight times more energy efficient by disc refining as compared with PFI mill refining, respectively. The results indicate that disc refining of hardwood is the most energy efficient method of nanocellulose production, and this outcome can be applied to predict and minimise mechanical energy consumption, and therefore cost and environmental impacts, for nanocellulose production.

1. Introduction

Energy is critical to the economic and social aspects of life. Most of the current world energy sources are based on fossil fuels, which are non-renewable and contribute to high greenhouse gas emissions (Monastersky, 2013). The rise in global temperatures and acceleration of climate change due to greenhouse effect has forced policy makers, ecologists and government bodies to target reduced dependency on fossil fuels. This creates a need for carbon neutral and sustainable routes toward cleaner production processes which can address energy security issues without adversely impacting the environment (Holzman, 2008).

Cellulose is renewable, biodegradable, non-toxic and abundant (Klemm et al., 2011). When cellulose fibers are broken down in nanoscale microfibrils, they can be used to produce a unique class of materials known as mechanically prepared nanocellulose (cellulose nanofiber i.e., CNF) which have high strength, high specific surface area, low toxicity, good biodegradability, and good barrier properties (Osong et al., 2016). Mechanically prepared nanocellulose, also known as nanofibrillated cellulose (CNF) is defined as having a high aspect ratio of > 100 (Bharimalla et al., 2015), with fiber diameter of 1−100 nm and length of 500−2000 nm (Abdul Khalil et al., 2014).

One potential large-scale application for nanocellulose is in paper sheet strength enhancement. Sheet strength is governed by fiber length, fiber bonded area, sheet formation and strength of fiber bonds (Taipale

* Corresponding author.
E-mail address: warren.batchelor@monash.edu (W. Batchelor).

https://doi.org/10.1016/j.indcrop.2021.113868
Received 15 April 2021; Received in revised form 22 July 2021; Accepted 25 July 2021
Available online 30 July 2021

et al., 2010). Pulp fines (particles that pass through a 200-mesh screen), produced during refining enhances the mechanical strength of sheets (Fischer et al., 2017). Nanocellulose fibers are a subset of fines. However, a high percentage of fines can result in high sheet drainage times, which decreases the production efficiency of a paper machine (Hubbe et al., 2017). Thus, in the papermaking process, there is a trade-off between the degree of refining (which adds to high energy and dewatering cost) and sheet strength development, while maintaining high productivity. Since there are numerous combinations of nanocellulose production methods available, it is crucial to characterise their impact on the fiber properties to determine the most productive, sustainable and energy efficient treatment.

Lignocellulose biomass has great potential for nanocellulose production due to its abundance, low cost and renewability (Lee et al., 2014). Some of the lignocellulosic biomass that has been reported for producing nanocellulose includes hardwoods (Zhang et al., 2021), softwoods (Iwamoto et al., 2008), banana rachis, pineapple leaf, sisal (Deepa et al., 2015), carrot waste (Varanasi et al., 2018), rice husks (Rashid and Dutta, 2020) and Alfa stem fibers (Marrakchi et al., 2011). Extraction of nanocellulose from cellulosic materials can involve an acid hydrolysis (Bondeson et al., 2006), enzymatic (Kaschuk et al., 2017), subcritical water hydrolysis (Novo et al., 2016) or TEMPO (2,2,6,6 -Tetramethylpiperidine 1-oxyl) oxidative (Isogai et al., 2011) pre-treatment to prepare the fibers, followed by mechanical treatment to facilitate size reduction (Pires et al., 2019). None of these chemical or oxidative pre-treatment methods are environmentally benign and also incurs extra costs as well increase chemical pollution. As an alternative, mechanical refining is an easy and effective method which does not use any chemicals or enzymes, minimises potential pollution and proposes a green solution for sustainable and scalable production of nanocellulose. Production of nanocellulose from corn stalks has been reported by use of a high-speed blender to highlight the possibility of scale up (Boufi and Chaker, 2016).

An ideal solution to reduce negative environmental impact for upgrading the value of industrial crop utilisation would be one that retains nanocellulose product performance while:

a) Removing the toxic chemical and oxidative pre-treatments
b) Lowering energy consumption
c) Using renewable cellulosic biomass sources

The most promising approach to meet all these performance requirements is a high-efficiency, purely mechanical process with minimal waste generation. Mechanical processes include refining (Kerekes, 2005) which can be used by itself (Jahangir and Olson, 2020) or as mechanical pre-treatment, followed by either high pressure homogenisation (Nakagaito and Yano, 2005), screw extrusion (Jonoobi et al., 2010), microfluidization (Pacaphol and Aht-Ong, 2017) or cryo-crushing and grinding (Siró and Plackett, 2010). Disc and conical refiners are the two most common pilot scale, low consistency (2−6 wt. % solids) refiners with bars on both rotor and stator, therefore producing higher shear. The nature of low consistency refining is defined by specific edge load (*SEL*), which is energy expended per unit length of bar crossing. Disc refiners are equipped with two parallel steel discs, the rotor with bars and the stator with grooves, which rotate in opposite directions, shearing and breaking the pulp fibers caught between them. The PFI (Papir Forsknings Institutet) mill, in contrast, works by rapidly applying shear and compressive forces using two parallel surfaces under constant load, leading to predominantly internal fibrillation (Kerekes, 2005). The energy of refining is dependent on the number of impacts, quantity and intensity of refining. A laboratory based PFI mill device and homogenisation is used to achieve high strength and high fibre aspect ratio and is not particularly designed to achieve energy efficient results. Isolation of nanocellulose from pulp has been investigated by high pressure homogenisation, however the energy consumption of was not reported (Wang et al., 2017). The specific energy consumption required for a dry grinding method (shear cutting mill) was shown to have lower specific energy consumption as compared with PFI mill refining. However, this method requires dried pulp samples which may be a limitation while scaling up nanocellulose production (Lee and Mani, 2017).

When considering life-cycle analysis of nanocellulose production processes, the sustainability and environmental impact have been questioned (Piccinno et al., 2018). The major barrier to commercialisation of nanocellulose, whether for stand-alone applications or as an additive in papermaking, is the high energy consumption required by mechanical treatment (Osong et al., 2016). Some of the high energy numbers associated with the production of nanocellulose using homogenisation are listed in Table 1. Most of the studies involve a pre-treatment method with subsequent mechanical refining for nanocellulose production (Osong et al., 2016).

However, despite advances in the field, current processes to produce nanocellulose remain energy intensive, with correspondingly high environmental impacts. A recent comparison of the embodied energy of nanocellulose sheets to PET films, showed that even if a relatively low energy consumption of 20,000 kW h/t was assumed for nanocellulose production, then the nanocellulose sheets had an embodied energy that was approximately double that of the PET films (Nadeem et al., 2020). Therefore, for the full potential of this material to be realized, there is a need to develop energy efficient nanocellulose production methods to improve its commercial viability and reduce the impacts of production.

Wood species are categorised as hardwood or softwood based on the differences in their cell wall structure (Stelte and Sanadi, 2009). Hardwood fibers tend to be shorter and thinner as compared with softwood fibers, and these differences may impact the efficiency and effectiveness of a particular mechanical treatment method to produce nanocellulose. Although previous studies have reported the effect of hydrothermal and enzymatic pretreatment followed by mechanical refining, these investigations were limited to using water at high temperature and expensive enzymes under batch conditions which represent significant limitations for making the process scalable and economically viable (Liu et al., 2020; Xu et al., 2020). Disc refining, on the other hand, is a purely mechanical process that does not require temperature adjustment, or enzymatic or chemical reactions to produce nanocellulose. Disc refining is a continuous pilot scale process that has the capability to simultaneously control degree of refining; enabling high quality nanocellulose at lower production cost.

There has been no study reported demonstrating and comparing the ability of hardwood and softwood fibers for mechanically prepared nanocellulose (CNF) production across lab (PFI mill and homogenisation) and pilot scale (disc) refiners which is precisely the aim of this work. This absence is significant given that hardwood and softwood pulp fibers are two of the most significant industrial crops worldwide. Fiber property development (aspect ratio, fines percentage, fiber diameter), sheet strength (tensile index, sheet density) and sheet production rate (drainage time) was measured and compared across two scales of refining to show the effect of fiber and refiner on scalability and energy efficiency for sustainable nanocellulose production. A novel quality index (Q) was developed to relate fines quality to fiber diameter and relative bonded area to quantify the relative process and energy efficiency of the nanocellulose production methods, highlighting the novelty and significance of this research. The quality index developed in this work has the potential to meet the future needs of nanocellulose users in paper strength and nanocomposite applications.

2. Materials and methods

2.1. Materials

Never dried, unrefined Australian Bleached Eucalyptus Kraft pulp (ABEK0) was supplied from Australian Paper Maryvale at 10 wt.%. Dried unrefined Brazilian Bleached Eucalyptus Kraft (BBEK0) sheets were supplied from Brazil. ABEK0 and BBEK0 were soaked overnight in

Table 1
Specific energy consumption of various pre-treatments applied to different source of pulp with homogenisation as mechanical treatment.

Type of pulp	Pretreatment type	Mechanical Treatment	Total Specific Energy Consumption (SEC) kWh/t	References
Bleached Eucalyptus	PFI mill refining	Homogenisation	39,309	(Ang et al., 2019)
Sulphite	No	Homogenisation	27,000	(Ankerfors, 2012)
Sugar Beet	No	Homogenisation	30,000	(Siró and Plackett, 2010)
Bleached Eucalyptus	*TEMPO	Homogenisation	10,000	(Syverud et al., 2011)
Kraft	Claflin Refining	Homogenisation	25,400	(Eriksen et al., 2008)
Kraft	Valley Beater	Homogenisation	22,000	(Spence et al., 2011)

* TEMPO: 2,2,6,6 -Tetramethylpiperidine 1-oxyl.

a 2 L beaker, then diluted to 1.2 wt.% and disintegrated at 15,000 revolutions in a 3 L Mavis Engineering Standard Disintegrator (Model 8522). The disintegrated pulp was concentrated to 10 wt.% using a Buchner funnel.

Unrefined Northern Bleached Softwood Kraft pulp (NBSK0) at 3.5 wt.% was supplied by the University of British Columbia (UBC), Canada. BBEK0 and NBSK0 samples were treated with both laboratory PFI mill refining at Monash University and pilot scale disc refining at UBC. NBSK0 pulp was disintegrated at 1400 rpm, 3.6 wt.% in a 250 L tank for 10 min, prior to disc refining. ABEK0 samples was treated with laboratory refining (PFI mill refining and homogenisation) only.

2.2. Lab scale PFI refining

Hardwood Australian (ABEK0) and Brazilian BEK (BBEK0) pulp was refined using a PFI mill, according to TAPPI standard 248 (TAPPI, 2001a). A PFI mill is a low consistency refiner that is mainly used in laboratory scale. ABEK and BBEK pulp at a solids content of approximately 10 wt.% were refined at 15,000, 30,000 and 50,000 revolutions, and the level of refining added to the sample name as shown in Table 2. After PFI refining, the samples were diluted to 1.2 wt.% solids, disintegrated for 15,000 revolutions in a 3 L Mavis Engineering standard disintegrator (Model No 8522), and used for sheet production. A subsample of ABEK50 K was further diluted to 0.5 wt.% solids and subjected to high pressure homogenisation (HPH) using a GEA Niro Soavi (Type: Pandaplus 2000) for three passes at 1000 bar.

Softwood NBSK pulp (NBSK0) was also refined in the PFI mill at 15,000, 30,000 and 50,000 revolutions, and the level of refining added to the sample name (Table 2). The laboratory scale mechanical energy consumption with PFI mill and homogenization was measured using a Hager EC350 Three-Phase kWh-meter.

2.3. Pilot scale mechanical refining

Hardwood BBEK0 pulp and Softwood NBSK0 pulp were refined in a 14-inch single disc LC Aikawa low consistency disc refiner located at The University of British Columbia (UBC). The UBC disc refiner is powered by a 112-kW motor. It uses a 30-kW centrifugal pump. Softwood pulp was refined to various levels in this disc refiner at a constant feed flow rate of 250 L/min and a consistency of 3.6 wt.%. The gap size for the no-load condition was 3.5 mm, and for the refining trial it was maintained in between 0.114−0.406 mm. The stock was recirculated until the desired energy input was reached. The specific edge load (*SEL*) was maintained at 0.6 J/m with a plate of bar edge length 2.74 km/rev operating with a horizontal rotational speed of 1200 rpm. All the operational refining parameters (flow rate readings, pressure, temperature indicator, gap clearance indicator, valve opening, pump frequency reading and refiner speed) were controlled using a computer interface (LabVIEW program).

The resulting fibers were labelled in order of increasing degree of refining from NBSK0 (unrefined) to NBSK11 (highly refined) and from BBEK0 to BBEK5 (Table 3).

Table 2
Naming conventions for PFI milling samples (ABEK, BBEK & NBSK).

Sample	PFI milling revolutions	Homogenisation passes at 1000 bar
ABEK0	0	0
ABEK15k	15,000	0
ABEK30k	30,000	0
ABEK50k	50,000	0
ABEK50k3P	50,000	3
BBEK0	0	0
BBEK15k	15,000	0
BBEK30k	30,000	0
BBEK50k	50,000	0
NBSK0	0	0
NBSK15k	15,000	0
NBSK30k	30,000	0
NBSK50k	50,000	0

2.4. Pilot scale specific energy consumption

The power of the UBC disc refiner was recorded by LabVIEW software, where net power (P_{net}) is the total power used by the refiner motors minus the no-load power (water flowing through the refiner). The specific energy consumption (*SEC*) measurement is then calculated as in (Eq. 1). Specific edge load (*SEL*), which is a measure of fiber treatment intensity, is calculated as the ratio of net power to the product of bar edge length (*BEL*) and motor rotational frequency (Eq. 2).

$$SEC = \frac{P\_net}{\dot{m}} \quad (1)$$

where *P_net* is net power consumption in (kW), and $\dot{m}$ is mass flow rate of dry fibers through refiners in (t/hour).

$$SEL = \frac{P\_net}{BEL^{*}(f)} \quad (2)$$

where *SEL* is in J/m; *P_net* is in kW; *BEL* (product of number of rotor and stator bars and contact length of opposite bars) is in km/rev; and *f* is rotational refiner motor frequency in revolutions per second. The level of refining, naming conventions, and treatment types for each sample produced in this study are summarized in Table 3.

2.5. SEM imaging and fiber diameter distribution

All fiber samples were first diluted to 0.001 wt.% and a single drop was cast on top of a silicon chip. The samples were then dried, and

Table 3
Naming conventions for disc refined NBSK and BBEK samples.

Sample	Refining time in disc refiner, seconds (s)	Sample	Refining time in disc refiner, seconds (s)
NBSK0	0	BBEK0	0
NBSK1	376	BBEK1	660
NBSK2	642	BBEK2	921
NBSK3	920	BBEK3	1673
NBSK4	1260	BBEK4	2442
NBSK6	1869	BBEK5	2652
NBSK9	3415		
NBSK11	3959		

iridium coated in preparation for SEM imaging. SEM images were then taken using a FEI Nova NanoSEM 450 FEG fitted with a monochromator at 5.00 kV voltage, spot size 2, and working distance of 5.0 mm. The image pixels were then calibrated with the length scale using ImageJ processing software. All observable fibers in each SEM image were counted manually. From high magnification images, nanocellulose fiber diameter (both BEK and NBSK samples) were sorted into 10–50 nm sized bins and then plotted and compared on a frequency versus bin range graph to show the effect of refining on diameter distribution. This methodology was adapted from previous research work (Ang et al., 2020).

2.6. Brecht-Holl fiber classification (screening)

An equivalent dry weight of 1−2 g was taken from wet BEK (both ABEK & BBEK) pulp (10−12 wt.%) and wet NBSK pulp (1–3.5 wt.%). The subsamples were diluted with water (≤ 1 wt.%) and mixed with Waring Commercial Immersion blender (WSB 33XNNA) for 1 min. Samples were classified using a Brecht-Holl 200 mesh screener. A dilution water flow rate of 2 L/min was maintained during classification and a water sparge was used to agitate the sample. Due to the high volume of water associated with the fines fraction, it is challenging to separate and quantify fines (Fischer et al., 2017). Hence long fibers were quantified in these trials. The coarse rejects, which did not pass through the mesh, were collected, dried and quantified. Where required, the screened fines fraction was quantified by difference.

2.7. Sedimentation and gel point measurement

Sedimentation tests were performed at concentrations ranging from 0.1 to 0.01 wt.% for each sample. Each sample was mixed using a Waring Commercial Immersion blender (WSB 33XNNA) for 1 min before being poured into a 250 mL measuring cylinder and allowed to settle under gravity for at least 48 h. The initial solids concentration was then plotted against the ratio of final sediment height (H_s) to initial sediment height (H_o) to determine the gel point of the suspension. The linear term of the fit of the graph determines the gel point of the suspension which is the lowest solids concentration at which fibers form a continuous network. The data of initial solids concentration (C_o) versus (H_s/H_o) was fitted with a smoothing spline (smoothing parameter of p = 0.998) in Matlab (Raj et al., 2016). The constant y intercept value at the origin of the first derivative curve represents gel point (S2.7).

2.8. Aspect ratio estimation

The gel point values obtained by sedimentation were used to calculate the aspect ratio of each fiber sample using Effective Medium Theory (EMT) assuming a cellulose density of 1333 kg/m^3 in water as per (Eq. 3) (Varanasi and Batchelor, 2013).

$$AR = 2.98{C_c}^{-0.58} \tag{3}$$

where AR is the aspect ratio of the fibers and C_c is the solids concentration at the gel point.

2.9. Laboratory handsheet making

All samples were disintegrated for 15,000 revolutions in a 3 L Mavis Engineering Standard Disintegrator (Model 8522). All hand sheets were prepared using a British Handsheet Maker (Model 8802). A 60 gsm handsheet was formed from 600 mL of a 0.2 wt.% suspension using GE Whatman Grade 541 filter paper (22 μm pore size) placed on a 150 mesh (104 μm pore size). Drainage time was measured and recorded from the start of automated drain cycle until the sheet was completely drained. Drained sheets were couched manually with blotting paper and carefully separated from the mesh and original filter paper. Sheets were then pressed at 345 kPa for 5 min in an automatic L&W sheet press (A B Lorentzen & Wettre, Model No 576). 3 circular hand sheet replicates were produced for each fiber sample and sheets were maintained at constant conditions (50 % relative humidity, 23 °C according to TAPPI T402 standards (TAPPI, 2001b) for 24 h prior to testing.

2.10. Handsheets characterization

Handsheets were cut into 15 mm wide strips using a sheet cutter (Delta Hydraulics CT01861B). Tensile tests were performed on an Instron 226 Model 5566 Universal Testing Machine at a constant elongation rate of 10 mm/min. At least 15 separate 10 cm strips from 3 replicate handsheet were measured for each fiber sample for each refining level. A load-displacement curve for each sample was recored (from which the maximum load was subsequently derived. The strength results were expressed as tensile index, which was calculated by dividing the maximum tensile load by the width of the strip (15 mm) and grammage of paper sheet (60 g/m^2). The mean sheet thickness was measured as an average of 20 random points for each sheet using descriptive statistics in an L&W Micrometer (Model No 51).

2.11. Quality index

The starting point of the quality index development is the recognition that bonded surface area within the sheet should control the properties. The pulp starting material is divided into two volume fractions: a fines/nanofiber fraction and a large fiber fraction. For the purposes of this analysis, it was assumed that only the fines volume fraction is contributing to the available surface area. This is a reasonable assumption at moderate to high fines/nanofiber levels. The fines volume fraction was denoted as v_{nf} and the large fiber fraction (v_f). The aspect ratio, which is measured from sedimentation was assumed to be the same for all the fibers. Using high magnification SEM images, the dimensions of a set of k fibers is measured and this set of k fibers is assumed to be representative of all the fines in that sample. A single fiber denoted i, which is part of the set of k fibers, has length l_i and diameter d_i, where $AR = l_i/d_i$. Assuming the fiber is cylindrical, the volume of this fiber is $V_i = \pi \left(\frac{d_i}{2}\right)^2 l_i = \frac{\pi}{4} {d_i}^3 AR$ and the mass of this fiber is $M_i = \frac{\pi}{4}{d_i}^3 AR\,\rho$, where ρ is cellulose fiber density (assumed to be 1500 kg/m^3). The relative bonded area (RBA) is the fraction of total available surface for bonding (Batchelor & He, 2005).

The total mass of a set of k fibers is $M_t = \frac{\pi}{4}\rho\, AR \sum_{i=1}^{i=k} di^3$ (4a)

Surface area of a single fiber i is $S_i = \pi d_i\, l_i + 2\pi\frac{di^2}{4}$, $S_i = \pi {d_i}^2\left(AR + \frac{1}{2}\right) = \pi di^2 AR$,

The total surface area of a set of k fibers is $S_t = \pi\, AR \sum_{i=1}^{i=k} di^2$ (4b)

The specific surface area of a set of k fibers is $SSA_k = \frac{S_t}{M_t} = \frac{\pi\, AR \sum_{i=1}^{i=k} di^2}{\frac{\pi}{4}\,\rho AR \sum_{i=1}^{i=k} di^3}$ (4c)

$$SSA = f\, SSA_k + (1-f)\, SSA_{long} \tag{4d}$$

Since large fibers have negligible surface area:

$$SSA = f\, SSA_k = f\frac{\pi\, AR \sum_{i=1}^{i=k} di^2}{\frac{\pi}{4}\,\rho AR \sum_{i=1}^{i=k} di^3} \tag{4e}$$

Relative bonded area (RBA) is the ratio of sheet density to cellulose density:

$$RBA = \frac{Sheet\ density}{Cellulose\ density} = \frac{\rho_{sheet}}{\rho} \quad (4f)$$

Finally, the Quality index, Q, is the product of the specific surface area and relative bonded area:

$$Q = 4f\ \frac{\sum_{i=1}^{i=k} di^2}{\rho \sum_{i=1}^{i=k} di^3}\ x\ \frac{\rho_{sheet}}{\rho} \quad (4g)$$

This quality index is a useful benchmarking tool for assessing the nanocellulose product development by different process conditions which highlights the significance of this research. The nanocellulose produced using any method consists of a mixture of fines and larger fibers. This combination impacts the resulting strength of a paper sheet produced from pulp, as strength depends on the bonding ability of the fiber network, which in turn depends on their dimensions and the starting fiber type. The quality index therefore provides a simple way to compare nanocellulose products from different production processes and pulp; thus, is a valuable tool in predicting quality.

2.12. Physicochemical characterisation: FTIR

Approximately 50 mg of oven-dried fibers were analyzed with a Fourier-Transform Infrared (FTIR) spectrometer (Agilent Technologies Cary 630 FTIR) equipped with a diamond ATR accessory. Five scans at 4cm^{-1} resolution were recorded in the range of 500−4000 cm^{-1}.

3. Results and discussion

It is necessary to develop a scalable method for sustainable nanocellulose production and correlation with energy efficiency must be demonstrated based on type of pulp (hardwood or softwood) and choice of refiner. An increase in number of revolutions or refining time obviously indicates an increase in energy consumption for fibrillation, however how the fiber and sheet property development shapes up, and which combination of pulp and refiner is most suitable for mass scale production of nanocellulose is yet to be explicitly quantified which highlights the novelty and innovation of this work.

3.1. Specific energy consumption (SEC)

The specific energy consumptions for BEK (ABEK and BBEK) and NBSK pulp samples refined by lab PFI mill and pilot disc refining methods are summarised in Eqs. 5a, 5b and 5c respectively, as functions of PFI revolutions and of refining time. The specific energy consumption equations are derived from the slope of measured specific energy consumption (SEC, kWh/t) versus refining level plotted in Fig S1a and Fig S1b. Fig (S1a).

$$E_{PFI} = 0.37\ r \quad (5a)$$

where E_{PFI} is Specific energy consumption of PFI mill refiner (kWh/t) and r is refining level (PFI mill revolutions x 10^3). Fig (S1b).

$$E_{disc\ NBSK} = 0.839\ t \quad (5b)$$

$$E_{disc\ BBEK} = 0.342\ t \quad (5c)$$

where E_{disc} is specific energy consumption of disc refiner (kWh/t) and t is disc refining time in seconds.

With increasing PFI mill revolutions, there is an increase in SEC. Both BEK (ABEK and BBEK) and NBSK samples had energy consumption of 17,417 kW h/t at 50,000 PFI revs. NBSK11 and BBEK5, the most heavily disc refined softwood and hardwood samples, had specific energy consumptions of 3346 kW h/t and 953 kW h/t, respectively. The maximum energy achievable for BBEK refining was determined by the pulp viscosity, which increased with increasing processing and therefore increasing energy, until the disc refiner clogged. The specific energy consumption measured for lab scale PFI mill refining was the average of three replicates for each refining level. Pilot disc refining was not replicated. During PFI mill operation, revolutions (displayed on PFI mill) taken as indicative of the level of refining (TAPPI, 2001a). However, during disc refining trial time (displayed on LabView software) is used as measure of degree of refining.

For laboratory PFI mill refining, the measured energy consumption was 0.37 kW h/t/rev for NBSK and BEK (ABEK & BBEK) samples (Eq. 5a, Fig S1a). This is substantially higher than the net energy consumption of 0.2 kW h/t/rev previously reported for bleached kraft pulp-eucalyptus wood species (Kerekes, 2005). Fig S1a also includes a data point for ABEK sample that was homogenised for 3 passes after 50k PFI mill refining. For pilot disc refining, the measured energy consumption was 0.839 kW h/t/s and 0.342 kW h/t/s for treating NBSK and BBEK respectively (Eqs. 5b and 5c, Fig S1b). Note that ABEK was not treated in the pilot disc refiner.

The measured energy consumption of 1 wt.% suspension of ABEK pulp homogenised for one pass at 1000 bar was 7200 kW h/t. This is significantly higher than previously reported (Ankerfors, 2012) because the pressure drop equation, which is a simplified form of Bernoulli's equation, does not consider design and size of the homogeniser, or the effect of pulp viscosity (Raj et al., 2016).

3.2. Fiber diameter distribution

With progressive refining there is peeling off of the outer cell wall layer of cellulose, which decreases the width of the fibers. SEM imaging and fiber diameter distribution using ImageJ can be used to quantify the nanoscale dimensions of fibers (Ang et al., 2020). This is important to characterise the material source, as well as the ways in which level and method of refining affect the fiber dimensions at nanoscale. To improve productivity and processing ability of both softwood and hardwood at laboratory and pilot scale, there is a need to understand how the fibrillation from micro to nanoscale is happening during mechanical treatment. Fiber diameter distributions of ABEK, BBEK and NBSK samples were determined from SEM images. Images of unrefined NBSK0 and ABEK0 (Fig. 1) were taken at an appropriate magnification to show at

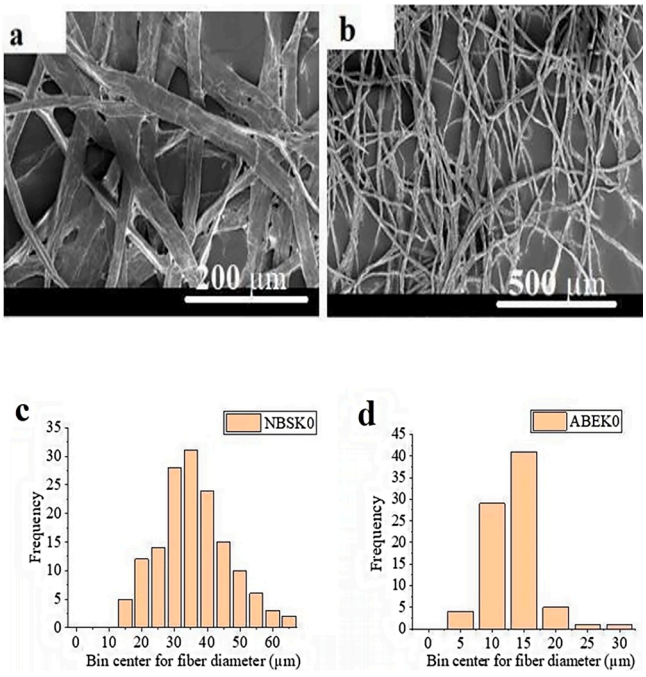

Fig. 1. SEM images of a) unrefined NBSK0, b) unrefined ABEK0, c) diameter distribution of unrefined NBSK0 and d) diameter distribution of unrefined ABEK0.

least 150–200 individual fibers in total in the microscopy field. Fig. 1a and b depict the SEM images while Fig. 1c and d represent the diameter distribution of unrefined NBSK0 and ABEK0, respectively. Fig. 2a and 2c shows the SEM images of moderately and highly disc refined NBSK while Fig. 2b and d represent that of moderately and highly lab refined ABEK fibers. The diameter distribution of disc refined NBSK and lab refined ABEK is compared in Fig. 3a and b, respectively. Similarly, the SEM images of disc and PFI mill refined BBEK are shown in Fig S2 whereas Fig S3 shows the SEM images of PFI mill refined NBSK samples. Comparison of fiber diameter distribution was also made between NBSK and ABEK samples both refined by PFI mill with similar energy consumption (Fig. 3c). A comparison between the fiber diameter distributions achieved by the most intensive PFI mill and disc refining treatments for the same NBSK sample was also made to study the impact of choice of refiners (Fig. 3d).

Higher specific energy consumption resulted in lower fiber diameters for a given mechanical treatment. Industrial disc refining required 3346 kW h/t to reduce the diameter range of NBSK fibers by almost 1000x from 30−40 μm (NBSK0) to 40−60 nm (NBSK11) (Figs. 1c and 3 a). In comparison, a combination of laboratory PFI mill refining and homogenization, consuming a total of 39,017 kW h/t, was required to achieve the same reduction in diameter of ABEK fibers (Figs. 1d and 3 b). Homogenisation had the greatest influence on ABEK fiber diameter, but showed the greatest specific energy consumption, with 3 passes at 1000 bar reducing the 70−100 nm diameter fibers (ABEK50k) to 40−60 nm diameter fibers (ABEK50k3P) consuming an additional 21,600 kW h/t (Fig. 3b). With the equivalent expenditure of 17,417 kW h/t energy in PFI refining, ABEK50k has much smaller individual and median fiber diameters compared with NBSK50k, as evident from the left shift of histogram plot (Fig. 3c). However, it took only 1600 kW h/t energy in the industrial disc refiner to produce the nanocellulose product NBSK6. NBSK11, which uses approximately a fifth of the energy required for the NBSK 50k sample, has much smaller fiber diameter (Fig. 3d).

Both methods of fiber diameter reduction achieved nanofibers with dimensions suitable for known nanocellulose applications such as filter and nanocomposite materials (Varanasi et al., 2015). However, the laboratory PFI mill plus homogenization method uses over 10x as much energy as pilot disc refining. Low consistency (i.e., disc) refining consumes much less energy than conventional high consistency refining, thus indicates the need for further research (Harirforoush et al., 2016).

3.3. Efficiency of the refining methods: Sedimentation and gel point determination

The results of sedimentation experiments of NBSK and BEK (ABEK and BBEK) samples (unrefined and most heavily refined) processed by disc and PFI mill refining are shown in Fig. 4. The details of all samples

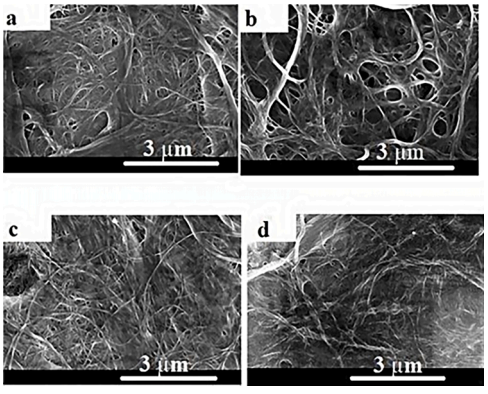

Fig. 2. SEM images of a) moderately disc refined NBSK (NBSK6), b) moderately lab refined ABEK (ABEK50k), c) highly disc refined NBSK (NBSK11), d) highly lab refined ABEK (ABEK50k3P).

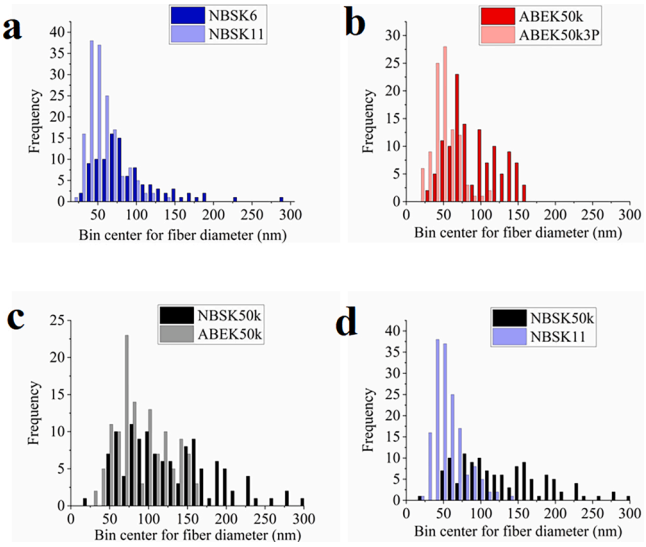

Fig. 3. Fiber diameter distribution of a) moderately disc refined NBSK (NBSK6) vs heavy disc refined NBSK (NBSK11) b) high PFI mill refined ABEK (ABEK50k) vs high PFI mill refined with 3 homogenisation passes (ABEK50k3P) c) heavily PFI mill refined NBSK (NBSK50k) vs heavily PFI mill refined ABEK (ABEK50k) and d) heavily PFI mill refined NBSK (NBSK 50k) vs heavily disc refined NBSK (NBSK11).

are shown in Fig S4 (a–e). The gel point is taken to be the slope of the linear fit of the data through the origin. The slope of aspect ratio versus energy consumption demonstrates the ease of processing of each sample.

From Fig. 4a, increasing the degree of mechanical refining gradually reduces the gel point of the fibers, indicated by the decreasing slope of the trendline. As expected, ABEK0 has the highest gel point (4.17 kg/m^3), and most highly refined fiber, ABEK50k has the lowest gel point (2.46 kg/m^3).

The rate of increase in aspect ratio and indicates increased ease of processing. The results of gel point determinations for unrefined and 50k refined ABEK, BBEK and NBSK treated by PFI mill and disc refining are presented in Fig. 4 (a–e). The trend for all samples is similar, with unrefined fibers showing consistently lower gel points than the more highly refined samples of the same fiber type, regardless of refining method, as expected.

The rate of reduction of gel point (or increase in aspect ratio) with mechanical energy consumption can be used to measure fiber processability and refining efficiency. The rate of increase in aspect ratio as a function of specific energy confirms that disc refining is seven times more energy efficient than PFI mill refining for processing softwood NBSK fibers and thirty-three times more efficient for processing hardwood BBEK fiber (determined by comparing the slope of the trendline for respective pulp and refiner in Fig. 4f).

Fibers being processed under shear can be either delaminated along the length or shortened or both. PFI mill treatment seems to have the two in balance, so aspect ratio stays approximately the same, after reaching threshold (around 100), however for disc refined NBSK, it was showing a linear increase which is because delamination was predominating over length reduction (Fig. 4f).

3.4. Development of fiber quality

Fines are the percentage of cellulose fiber material passing through a 200-mesh screen and include both nanofiber and larger fragments. The fines fraction is used to indicate the proportion of the feedstock that has been converted to nanocellulose, and therefore to indicate the quality of the mechanically treated product. In the current work, mechanically treated samples were separated into long fibers and fines by Brecht-Holl screening and fines were quantified by difference based on the mass of

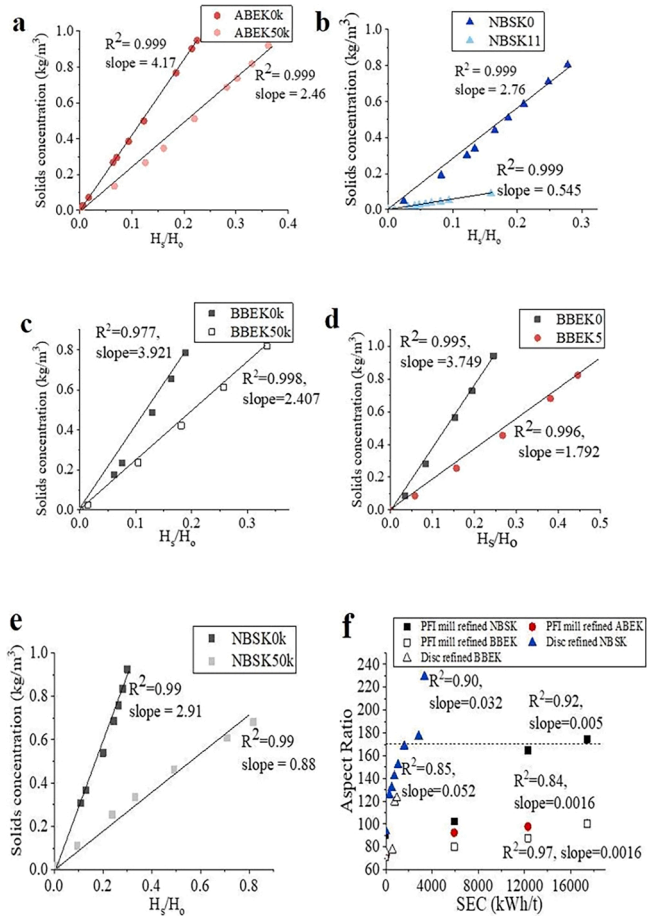

Fig. 4. Sedimentation behaviour (Spline fitted plots) of unrefined and highly refined a) PFI mill refined (0 kW h/t and 17,417 kW h/t) ABEK b) Disc refined NBSK (0 kW h/t and 3346 kW h/t) c) PFI mill refined BBEK (0 kW h/t and 17,417 kW h/t) d) Disc refined BBEK (0 kW h/t and 953 kW h/t) e) PFI mill refined NBSK (0 kW h/t and 17,417 kW h/t) f) Aspect ratio of PFI mill refined NBSK, PFI mill refined ABEK, PFI mill refined BBEK and Disc refined NBSK, Disc refined BBEK vs SEC.

long fibers retained on the screen. Fines fraction increased with increasing mechanical energy input for all combinations of fiber and mechanical energy treatment (Fig. 5a). The data also shows that the two sources of BEK hardwood fibers are much easier to break down than the larger NBSK softwood fibers, and that the industrial disc refining is more efficient (produces a higher fines fraction in the final product) than the laboratory PFI mill refining. It takes around 12,292 kW h/t of SEC to generate 80.5 % of fines from ABEK and 37 % fines from NBSK in PFI mill refining, however it takes only 1599.9 kW h/t of SEC to generate 76 % fines from NBSK in disc refining (Fig. 5a).

To achieve approximately 50 % fines in BBEK, disc refining consumes only 563 kW h/t of SEC which is an order of magnitude lower than that required by PFI mill refining (7760 kW h/t) (Fig. 5a, dotted line). This demonstrates the higher energy efficiency of disc refining over PFI mill refining. For a given combination of sample and mechanical treatment, fines generation during refining correlates well with aspect ratio development (Fig. 5b).

A comparison of the relationship between fines enhancement and specific energy consumption (SEC) across different pulp and refiner types shows that fines generation process efficiency follows the order Disc BBEK > Disc NBSK > PFI BBEK = ABEK > PFI NBSK.

Hand sheets were formed to further quantify the fiber quality and determine its potential impact on paper performance, as well as paper production efficiency. The results indicate that fibers of the size scale

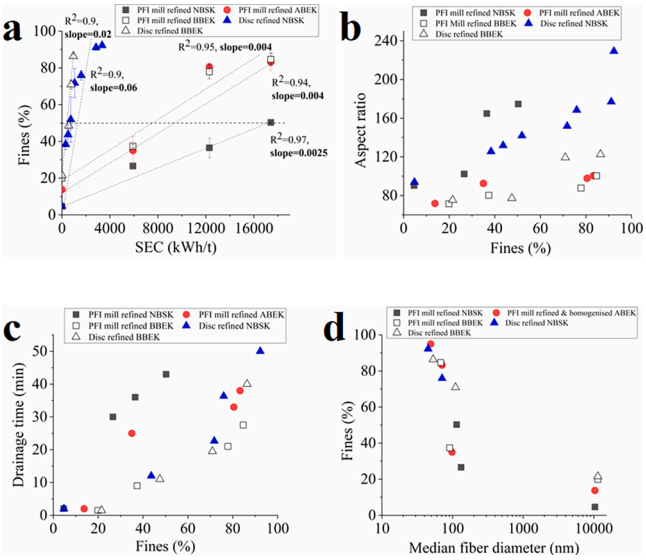

Fig. 5. a) Fines (%) recovered by Brecht Holl screening as a function of a) SEC b) Aspect Ratio as a function of fines, c) Drainage time as a function of fines, d) Fines vs Median fiber diameter.

and distribution produced by the current mechanical treatment methods can significantly increase the sheet drainage time, and therefore may impact paper production efficiency (Fig. 5c). A related decrease in fiber diameter also occurs during mechanical treatment (Fig. 5d), which decreases pore size and porosity during drainage resulting in significantly higher drainage resistance.

The relationships between SEC and tensile index, sheet density and sheet drainage time are given in Fig. 6a-c. From Fig. 6a, refined hand sheets (SEC > 0) from all fiber sources showed between three- to five-fold strength improvement over conventional unrefined fiber sheets (SEC = 0). Sheet density also increased with increased refining and higher SEC (Fig. 6b). Fig. 6c shows that increasing energy input to increase refining has a detrimental effect on drainage time, which

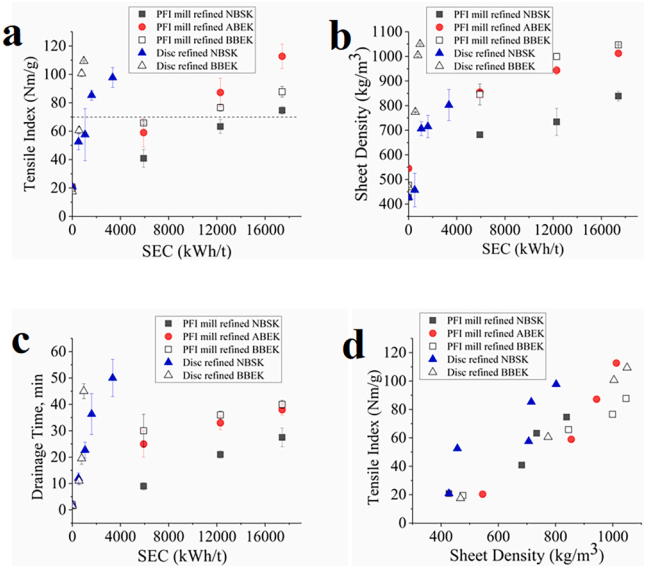

Fig. 6. Relationships between refining energy input (SEC) and the physical properties of Disc refined NBSK and BBEK, and PFI mill refined NBSK ABEK and BBEK a) SEC vs Tensile Index b) SEC vs Sheet Density c) SEC vs Drainage time d) and sheet density vs tensile index.
Note: initial data point for PFI mill refined NBSK and Disc refined NBSK are overlaid.

correlates with the increase in fines and decrease in pore size and porosity of the sheet and matches the results shown in Fig. 5c. There is a good general correlation between sheet density and tensile index (Fig. 6d), with sheets of higher density generally demonstrating higher strength, as expected, due to the increase in fiber surface area available for bonding.

Interestingly, both PFI mill refined hardwood samples (ABEK and BBEK) showed higher tensile index (Fig. 6a) and sheet density (Fig. 6b) compared to PFI mill refined NBSK (softwood) sheets. This may be due to the inherent nature of the wood species, and the modes of harvesting and plantation. In contrast, the sheet density of both ABEK and BBEK samples was very similar (Fig. 6b). Disc refining showed superior strength development when compared with PFI mill (Fig. 6a). The high energy efficiency of disc refining is due to the higher mechanical impact per refiner bar applied to fibers. Softwood fibers are longer and wider, whereas hardwood fibers are shorter and thinner. For similar tensile index (strength development of the NBSK pulp, PFI mill refining requires approximately ten times more energy than disc refining as shown in Fig. 6a.

The drainage time, which is less than 1 min for unrefined sheets, increases to up to an hour (Fig. 6c) with refining. This is due to the generation of pulp fines and consequential reduction in median fiber diameter (Fig. 5c and d). This extended drainage time would most likely be unacceptable in a commercial papermaking process. Therefore, there exists a balance between improving fiber quality to improve sheet properties and developing a commercial viability sheet forming process.

3.5. Quality index, Q

In order to show the relationship between energy input and fiber quality, a quality index, *Q*, was developed based on the relative bonded area (Batchelor and He, 2005), which is directly related to the fiber dimensions.

Fig. 7a shows the relationship between specific energy consumption and *Q*. All samples showed an approximately linear increase in *Q* with specific energy consumption. The slope of the plot of *Q* is therefore approximately proportional to the efficiency of the process. Refining decreases median fiber diameter thus increasing fiber specific surface area while also increasing the weight of fine material (Fig. 7b, c). As unrefined fibers are exposed to refining there is peeling of cell wall layers which enhances the bonding ability of fibers (due to exposed fiber-fiber OH functional groups), increasing *Q* (Fig. 7d).

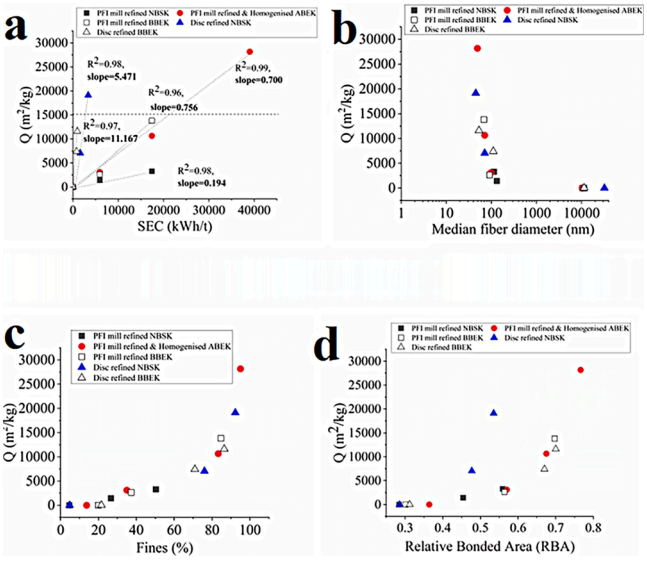

Fig. 7. Quality index as a function of a) SEC b) Median fiber diameter c) Fines and d) Relative Bonded area.

A decrease in median fiber diameter from micron to nanometre scale is correlated well with approximately three-fold improvement in *Q* (Fig. 7b). *Q* also increases linearly with increase in fines which correlates well with the increase in relative bonded area. The highest *Q* of 28,172 m^2/kg was from ABEK50K3P (PFI and homogenisation) requiring 39,017 kW h/t SEC. However, it took only 953 kW h/t of SEC to develop a quality index of 11,609 m^2/kg at 87 % fines for BBEK5 during industrial refining (Fig. 7c). An RBA of above 0.5 gave significant improvement in quality (Fig. 7d).

In terms of the combination of refining and fiber type, PFI mill refining of NBSK showed the lowest increase in Q for a given increase in SEC (0.194), while the increase in *Q* for the same energy input and refining method for ABEK (0.70) and BBEK (0.75) were significantly larger. Disc refined NBSK and BBEK gave specific *Q* increases relative to SEC input of 5.47 and 11.16, respectively. This demonstrates that disc refining of NBSK and BBEK is approximately twenty-eight times and fifteen times, respectively, more energy efficient at obtaining a similar quality of fiber than lab scale PFI mill refining. A comparison between best case scenario (BBEK disc refining) and worst-case scenario (NBSK PFI mill refining) shows that disc refining of BBEK is approximately fifty-eight times more energy efficient than PFI mill refining of NBSK (comparing slope of trendline Fig. 7a). Thus, BBEK and disc refining are the best combination of pulp and refiner type for the energy efficient production of nanocellulose. This is because hardwood which shows promising results against softwood if treated in disc pilot scale refiner (as compared with PFI mill) the energy consumption per ton of pulp goes down because of the uniform shear force distribution between the fibers. Disc refining is more energy efficient than PFI mill refining because of a more controllable and uniform plate gap which allows more homogenous distribution of shear force (increasing number of impact and intensity of each impact); main reason behind higher fiber intensity and energy efficient transfer. The plate design in disc refiner is done in such a way that refiner efficiency is higher (Luukkonen et al., 2012).

As a result of shear and compressive forces applied during homogenisation, the outer cell wall layer of cellulose fiber is peeled off, leading to both fiber diameter and sometimes length reduction. This process leads to generation of fines, and exposes additional surface area for bonding, increasing the density of the fiber network formed in sheets made from homogenised pulp. SEM fiber diameter distribution, fines percentage, aspect ratio, sheet strength and quality index development are all major attributes of quality development for mechanically prepared nanocellulose which forms the basis of our characterisation. While the fiber diameter, fines %, fiber aspect ratio, and sheet strength were measured, the fiber quality index was derived for the first time in this research that considers both fiber quality (fines, diameter, aspect ratio) and sheet strength (sheet density); giving an improved overall indication of nanocellulose fiber quality. Fines, fiber diameter, and fiber aspect ratio are all dependent on the extent of mechanical treatment and have been plotted together to show that mechanical treatment affects all three parameters simultaneously (Fig. 5b, c, d). However, mechanical treatment does not affect the physicochemical composition of nanocellulose product which is evident from FTIR results (Fig S5).

Comparatively low yielding laboratory scale nanocellulose production systems and deteriorating energy efficiency needed a sustainable route of production, which is now developed and amply evaluated. A new era of large scale, energy and cost-efficient production is on the offering which can pave the way for safe and sustainable agriculture and crop production. To reach a quality index of approximately 15,000 m^2/kg, the required specific energy consumption of the refiner-pulp combinations tested in this work follows the order Disc BBEK (1300 kW h/t)> Disc NBSK (2728 kW h/t)> PFI BBEK (19,737 kW h/t)> PFI ABEK (21,429 kW h/t)> PFI NBSK (77,320 kW h/t) which process and material efficiency (dotted line, Fig. 7a).

The disc refining of bleached eucalyptus kraft will also substantially reduce the embodied energy to under that of PET films by approximately twenty-five times (Jackson and Tamás, 2006). The disc refining process

requires no additional chemicals, especially no toxic catalysts, such as TEMPO (Fukuzumi et al., 2009). Overall, in context of industrial crop management principles, disc refining can be considered as an effective, safe, environmentally friendly method for sustainable and economical nanocellulose production.

4. Conclusion

Two refiners were compared based on the specific energy consumption required to process softwood and hardwood samples. A quality index based on fiber dimensions was used to assess each sample and refiner type as a function of refining energy consumption. The goal of the present work is to understand, quantitatively and qualitatively, the effect of choice of pulp, the difference in action between disc and PFI mill refiner and attain a better understanding of the nanocellulose quality development versus refining energy consumption across lab and pilot scale mechanical treatment.

PFI mill refining followed by 3 homogenisation passes showed a refining energy efficiency of approximately one-tenth of that of a disc refiner. However, PFI mill refined fiber showed improved sheet strength. In terms of quality index, disc refining of hardwood was fifty-eight times more energy efficient than PFI mill refining of softwood for a comparable product quality. This study confirms that while a combination of PFI mill refining and homogenisation produces a high-quality product with a small fiber diameter and high aspect ratio, this method is not energy efficient. Softwood and hardwood samples were subjected to different degrees of refining in a PFI mill and a disc refiner, and the fiber product quality was related to the energy consumption in each case. The degree of fiber refining was correlated with fiber properties, sheet strength development, and a newly developed fiber quality index. For the same method and degree of refining, softwood fibers showed a higher aspect ratio and lower sheet strength, and correspondingly lower quality index and fines percentages as compared with hardwood fibers.

To advance the commercial production of nanocellulose, an industrial crop product, it is critical that energy cost to performance trade-off is properly understood to design and select more efficient refiners. One way to achieve this, as this research shows, is disc refining of hardwood pulp. This work highlights the significance and potential of this green, clean and sustainable technique by optimising product quality and refining energy. The promising future of disc refining of hardwood pulp for larger scale nanocellulose production and applications was shown, which could facilitate waste management, enhance energy restoration, and provide a clean and sustainable material to replace fossil-based polymer products.

CRediT authorship contribution statement

Wriju Kargupta: Conceptualization, Methodology, Investigation, Formal analysis, Writing - original draft, Writing - review & editing. **Reanna Seifert:** Investigation, Methodology, Data acquisition. **Mark Martinez:** Resources & Investigation. **James Olson:** Resources & Investigation. **Joanne Tanner:** Conceptualization, Supervision, Project administration, Funding acquisition. **Warren Batchelor:** Conceptualization, Writing - review & editing, Supervision, Project administration, Funding acquisition.

Declaration of Competing Interest

The authors report no declarations of interest.

Acknowledgments

We wish to thank Australian Paper Maryvale for providing Bleached Eucalyptus pulp. Wriju Kargupta thanks Monash University for CF-MGS scholarship. The authors would like to acknowledge the facilities used with Monash Center for Electron Microscopy. We would also like to acknowledge the financial support from the Australian Research Council, Opal, Norske Skog and Visy through the Processing Advanced Lignocellulosics Industry Transformation Research Hub.

Appendix A. Supplementary data

Supplementary material related to this article can be found, in the online version, at doi:https://doi.org/10.1016/j.indcrop.2021.113868.

References

Abdul Khalil, H.P.S., Davoudpour, Y., Islam, M.N., Mustapha, A., Sudesh, K., Dungani, R., Jawaid, M., 2014. Production and modification of nanofibrillated cellulose using various mechanical processes: a review. Carbohydr. Polym. 99, 649–665. https://doi.org/10.1016/j.carbpol.2013.08.069.

Ang, S., Haritos, V., Batchelor, W., 2019. Effect of refining and homogenization on nanocellulose fiber development, sheet strength and energy consumption. Cellulose 26, 4767–4786. https://doi.org/10.1007/s10570-019-02400-5.

Ang, S., Narayanan, J.R., Kargupta, W., Haritos, V., Batchelor, W., 2020. Cellulose nanofiber diameter distributions from microscopy image analysis: effect of measurement statistics and operator. Cellulose 27, 4189–4208. https://doi.org/10.1007/s10570-020-03058-0.

Ankerfors, M., 2012. Microfibrillated Cellulose: Energy-Efficient Preparation Techniques and Key Properties. KTH Royal Institute of Technology.

Bharimalla, A.K., Deshmukh, S.P., Patil, P.G., Vigneshwaran, N., 2015. Energy efficient manufacturing of nanocellulose by chemo-and bio-mechanical processes: a review. World J. Nanosci. Eng. 5, 204. https://doi.org/10.4236/wjnse.2015.54021.

Bondeson, D., Mathew, A., Oksman, K., 2006. Optimization of the isolation of nanocrystals from microcrystalline cellulose by acid hydrolysis. Cellulose 13, 171. https://doi.org/10.1007/s10570-006-9061-4.

Boufi, S., Chaker, A., 2016. Easy production of cellulose nanofibrils from corn stalk by a conventional high speed blender. Ind. Crop. Prod. 93, 39–47. https://doi.org/10.1016/j.indcrop.2016.05.030.

Deepa, B., Abraham, E., Cordeiro, N., Mozetic, M., Mathew, A.P., Oksman, K., Faria, M., Thomas, S., Pothan, L.A., 2015. Utilization of various lignocellulosic biomass for the production of nanocellulose: a comparative study. Cellulose 22, 1075–1090. https://doi.org/10.1007/s10570-015-0554-x.

Eriksen, Ø., Syverud, K., Gregersen, Ø., 2008. The use of microfibrillated cellulose produced from kraft pulp as strength enhancer in TMP paper. Nord. Pulp Paper Res. J. 23, 299–304. https://doi.org/10.3183/npprj-2008-23-03-p299-304.

Fischer, W.J., Mayr, M., Spirk, S., Reishofer, D., Jagiello, L.A., Schmiedt, R., Colson, J., Zankel, A., Bauer, W., 2017. Pulp fines—characterization, sheet formation, and comparison to microfibrillated cellulose. Polym. 9, 366. https://doi.org/10.3390/polym9080366.

Fukuzumi, H., Saito, T., Iwata, T., Kumamoto, Y., Isogai, A., 2009. Transparent and high gas barrier films of cellulose nanofibers prepared by TEMPO-Mediated oxidation. Biomacromolecules. 10, 162–165. https://doi.org/10.1021/bm801065u.

Harirforoush, R., Wild, P., Olson, J., 2016. The relation between net power, gap, and forces on bars in low consistency refining. Nord. Pulp Pap. Res. J. 31, 71–78. https://doi.org/10.3183/npprj-2016-31-01-p071-078.

Holzman, D.C., 2008. The carbon footprint of biofuels: can we shrink it down to size in time? Environ. Health Perspect. 116 (6), 246–252. https://doi.org/10.1289/ehp.116-a246.

Hubbe, M.A., Ferrer, A., Tyagi, P., Yin, Y., Salas, C., Pal, L., Rojas, O.J., 2017. Nanocellulose in thin films, coatings, and plies for packaging applications: A review. BioResources. 12, 2143–2233.

Isogai, A., Saito, T., Fukuzumi, H., 2011. TEMPO-oxidized cellulose nanofibers. Nanoscale 3, 71–85. https://doi.org/10.1039/C0NR00583E.

Iwamoto, S., Abe, K., Yano, H., 2008. The Effect of Hemicelluloses on Wood Pulp Nanofibrillation and Nanofiber Network Characteristics. Biomacromolecules. 9, 1022–1026. https://doi.org/10.1021/bm701157n.

Jackson, S., Tamás, Bertény, 2006. Recycling of Plastics ImpEE Project, Department of Engineering. University of Cambridge.

Jahangir, E.S., Olson, J.A., 2020. Low consistency refined ligno-cellulose microfibre: an MFC alternative for high bulk, tear and tensile mechanical pulp papers. Cellulose 27, 2803–2816. https://doi.org/10.1007/s10570-019-02956-2.

Jonoobi, M., Harun, J., Mathew, A.P., Oksman, K., 2010. Mechanical properties of cellulose nanofiber (CNF) reinforced polylactic acid (PLA) prepared by twin screw extrusion. Compos. Sci. Technol. 70, 1742–1747. https://doi.org/10.1016/j.compscitech.2010.07.005.

Kaschuk, J.J., Lacerda, T.M., Coma, V., Frollini, E., 2017. Enzymatic hydrolysis of mercerized and unmercerized sisal pulp. Cellulose 24, 2437–2453. https://doi.org/10.1007/s10570-017-1284-z.

Kerekes, R.J., 2005. Characterizing refining action in PFI mills. Tappi J 2002 (4), 9–13.

Klemm, D., Kramer, F., Moritz, S., Lindström, T., Ankerfors, M., Gray, D., Dorris, A., 2011. Nanocelluloses: a new family of nature-based materials. Appl. Chem. Int. Ed. 50, 5438–5466. https://doi.org/10.1002/anie.201001273.

Lee, H., Mani, S., 2017. Mechanical pretreatment of cellulose pulp to produce cellulose nanofibrils using a dry grinding method. Ind. Crop. Prod. 104, 179–187. https://doi.org/10.1016/j.indcrop.2017.04.044.

Lee, H.V., Hamid, S.B.A., Zain, S.K., 2014. Conversion of Lignocellulosic Biomass to Nanocellulose: Structure and Chemical Process. Sci. World J. 2014, 631013 https://doi.org/10.1155/2014/631013.

Liu, X., Jiang, Y., Wang, L., Song, X., Qin, C., Wang, S., 2020. Tuning of size and properties of cellulose nanofibers isolated from sugarcane bagasse by endoglucanase-assisted mechanical grinding. Ind. Crop. Prod 146, 112201. https://doi.org/10.1016/j.indcrop.2020.112201.

Luukkonen, A., Olson, J., Martinez, D.M., 2012. Mechanical pulping: low consistency refining of mechanical pulp: relationships between refiner operating conditions and pulp properties. Nord. Pulp Paper Res. J. 27, 882–885. https://doi.org/10.3183/npprj-2012-27-05-p882-885.

Marrakchi, Z., Khiari, R., Oueslati, H., Mauret, E., Mhenni, F., 2011. Pulping and papermaking properties of Tunisian Alfa stems (Stipa tenacissima)—Effects of refining process. Ind. Crop. Prod. 34, 1572–1582. https://doi.org/10.1016/j.indcrop.2011.05.022.

Monastersky, R., 2013. Global carbon dioxide levels near worrisome milestone. Nat. 497, 13–14. https://doi.org/10.1038/497013a.

Nadeem, H., Naseri, M., Shanmugam, K., Dehghani, M., Browne, C., Miri, S., Garnier, G., Batchelor, W., 2020. An energy efficient production of high moisture barrier nanocellulose/carboxymethyl cellulose films via spray-deposition technique. Carbohydr. Polym. 250, 116911 https://doi.org/10.1016/j.carbpol.2020.116911.

Nakagaito, A.N., Yano, H., 2005. Novel high-strength biocomposites based on microfibrillated cellulose having nano-order-unit web-like network structure. Appl. Phys. A. 80, 155–159. https://doi.org/10.1007/s00339-003-2225-2.

Novo, L.P., Bras, J., García, A., Belgacem, N., Curvelo, A.Ad.S., 2016. A study of the production of cellulose nanocrystals through subcritical water hydrolysis. Ind. Crop. Prod. 93, 88–95. https://doi.org/10.1016/j.indcrop.2016.01.012.

Osong, S.H., Norgren, S., Engstrand, P., 2016. Processing of wood-based microfibrillated cellulose and nanofibrillated cellulose, and applications relating to papermaking: a review. Cellulose 23, 93–123. https://doi.org/10.1007/s10570-015-0798-5.

Pacaphol, K., Aht-Ong, D., 2017. Preparation of hemp nanofibers from agricultural waste by mechanical defibrillation in water. J. Clean. Prod. 142, 1283–1295. https://doi.org/10.1016/j.jclepro.2016.09.008.

Piccinno, F., Hischier, R., Seeger, S., Som, C., 2018. Predicting the environmental impact of a future nanocellulose production at industrial scale: Application of the life cycle assessment scale-up framework. J. Clean. Prod. 174, 283–295. https://doi.org/10.1016/j.jclepro.2017.10.226.

Pires, J.R.A., Souza, V.G.L., Fernando, A.L., 2019. Valorization of energy crops as a source for nanocellulose production – Current knowledge and future prospects. Ind. Crop. Prod. 140, 111642 https://doi.org/10.1016/j.indcrop.2019.111642.

Raj, P., Mayahi, A., Lahtinen, P., Varanasi, S., Garnier, G., Martin, D., Batchelor, W., 2016. Gel point as a measure of cellulose nanofibre quality and feedstock development with mechanical energy. Cellulose 23, 3051–3064. https://doi.org/10.1007/s10570-016-1039-2.

Rashid, S., Dutta, H., 2020. Characterization of nanocellulose extracted from short, medium and long grain rice husks. Ind. Crop. Prod. 154, 112627 https://doi.org/10.1016/j.indcrop.2020.112627.

Siró, I., Plackett, D., 2010. Microfibrillated cellulose and new nanocomposite materials: a review. Cellulose 17, 459–494. https://doi.org/10.1007/s10570-010-9405-y.

Spence, K.L., Venditti, R.A., Rojas, O.J., Habibi, Y., Pawlak, J.J., 2011. A comparative study of energy consumption and physical properties of microfibrillated cellulose produced by different processing methods. Cellulose 18, 1097–1111. https://doi.org/10.1007/s10570-011-9533-z.

Stelte, W., Sanadi, A.R., 2009. Preparation and characterization of cellulose nanofibers from two commercial hardwood and softwood pulps. Ind. Eng. Chem. Res. 48, 11211–11219. https://doi.org/10.1021/ie9011672.

Syverud, K., Chinga-Carrasco, G., Toledo, J., Toledo, P.G., 2011. A comparative study of Eucalyptus and Pinus radiata pulp fibres as raw materials for production of cellulose nanofibrils. Carbohydr. Polym. 84, 1033–1038. https://doi.org/10.1016/j.carbpol.2010.12.066.

Taipale, T., Österberg, M., Nykänen, A., Ruokolainen, J., Laine, J., 2010. Effect of microfibrillated cellulose and fines on the drainage of kraft pulp suspension and paper strength. Cellulose 17, 1005–1020. https://doi.org/10.1007/s10570-010-9431-9.

TAPPI, 2001a. T 248 sp-00 Laboratory Beating of Pulp (PFI Mill Method). Technical Association of the Pulp and Paper Industry (TAPPI) Press, Technology Park, Atlanta, GA, USA.

TAPPI, 2001b. T 402 sp-98 Standard Conditioning and Testing Atmospheres for Paper, Board, Pulp Handsheets, and Related Products. Technical Association of the Pulp and Paper Industry (TAPPI) Press, Technology Park, Atlanta, GA, USA.

Varanasi, S., Batchelor, W.J., 2013. Rapid preparation of cellulose nanofibre sheet. Cellulose 20, 211–215. https://doi.org/10.1007/s10570-012-9794-1.

Varanasi, S., Low, Z.-X., Batchelor, W., 2015. Cellulose nanofibre composite membranes – Biodegradable and recyclable UF membranes. Chem. Eng. J. 265, 138–146. https://doi.org/10.1016/j.cej.2014.11.085.

Varanasi, S., Henzel, L., Sharman, S., Batchelor, W., Garnier, G., 2018. Producing nanofibres from carrots with a chemical-free process. Carbohydr. Polym. 184, 307–314. https://doi.org/10.1016/j.carbpol.2017.12.056.

Wang, Y., Wei, X., Li, J., Wang, F., Wang, Q., Zhang, Y., Kong, L., 2017. Homogeneous isolation of nanocellulose from eucalyptus pulp by high pressure homogenization. Ind. Crop. Prod. 104, 237–241. https://doi.org/10.1016/j.indcrop.2017.04.032.

Xu, K., Shi, Z., Lyu, J., Zhang, Q., Zhong, T., Du, G., Wang, S., 2020. Effects of hydrothermal pretreatment on nano-mechanical property of switchgrass cell wall and on energy consumption of isolated lignin-coated cellulose nanofibrils by mechanical grinding. Ind. Crop. Prod. 149, 112317 https://doi.org/10.1016/j.indcrop.2020.112317.

Zhang, Q., Ma, R., Ma, L., Zhang, L., Fan, Y., Wang, Z., 2021. Contribution of lignin in esterified lignocellulose nanofibers (LCNFs) prepared by deep eutectic solvent treatment to the interface compatibility of LCNF/PLA composites. Ind. Crop. Prod. 166, 113460 https://doi.org/10.1016/j.indcrop.2021.113460.